AIP | Review of Scientific Instruments

Multiwell micromechanical cantilever array reader for biotechnology

R. Zhang, A. Best, R. Berger, S. Cherian, S. Lorenzoni, E. Macis, R. Raiteri, and R. Cain

Citation: Review of Scientific Instruments **78**, 084103 (2007); doi: 10.1063/1.2775433
View online: http://dx.doi.org/10.1063/1.2775433
View Table of Contents: http://scitation.aip.org/content/aip/journal/rsi/78/8?ver=pdfcov
Published by the AIP Publishing

Multiwell micromechanical cantilever array reader for biotechnology

R. Zhang,[a] A. Best, and R. Berger[b]
Max Planck Institute for Polymer Research, Ackermannweg 10, D-55128 Mainz, Germany

S. Cherian,[c] S. Lorenzoni, E. Macis, and R. Raiteri[d]
Department of Biophysical and Electronic Engineering, University of Genova, via all'Opera Pia 11a, I-16145 Genova, Italy

R. Cain[e]
Protiveris, Inc., 15010 Broschar Road, Rockville, Maryland 20850

(Received 29 May 2007; accepted 29 July 2007; published online 29 August 2007)

We use a multiwell micromechanical cantilever sensor (MCS) device to measure surface stress changes induced by specific adsorption of molecules. A multiplexed assay format facilitates the monitoring of the bending of 16 MCSs in parallel. The 16 MCSs are grouped within four separate wells. Each well can be addressed independently by different analyte liquids. This enables functionalization of MCS separately by flowing different solutions through each well. In addition, each well contains a fixed reference mirror which allows measuring the absolute bending of MCS. In addition, the mirror can be used to follow refractive index changes upon mixing of different solutions. The effect of the flow rate on the MCS bending change was found to be dependent on the absolute bending value of MCS. Experiments and finite element simulations of solution exchange in wells were performed. Both revealed that one solution can be exchanged by another one after 200 μl volume has flown through. Using this device, the adsorption of thiolated DNA molecules and 6-mercapto-1-hexanol on gold surfaces was performed to test the nanomechanical response of MCS. © *2007 American Institute of Physics.* [DOI: 10.1063/1.2775433]

I. INTRODUCTION

Micromechanical cantilever sensors (MCSs) are a new class of extremely sensitive sensor devices currently developed for chemical and biological detection.[1–6] MCS transduce recognition events on their receptor-coated surfaces into nanomechanical deflections. Interactions among a wide range of substances, including polymers, antibodies, proteins, cells, and drugs, can be studied.[7,8] There are several advantages of MCS over other sensing mechanisms: label-free detection of molecules, high sensitivity, high reproducibility,[9] and massive parallel measurements.[10]

MCS responses are sensitive to the unspecific adsorption of molecules from the environment and slow electrochemical processes such as silicon hydration. It is therefore mandatory to have a differential measurement configuration, where the reference MCS, coated with a layer inert to the analyte of interest, compensates all interfering interactions and thermal drift. Additionally, the sensitivity may vary from one MCS to another because of variations in the physical (e.g., thickness of the MCS and the deposited layers) and biochemical (e.g., density of the bioreceptors immobilized) characteristics. These variations can arise in the fabrication and functionalization processes of MCSs. Averaging the deflection response over several nominally identical MCSs increase the reliability of measurements.[11] Therefore MCS arrays are fabricated and used for sensing. MCS arrays with two,[12] four,[13] and eight[14] rectangular cantilevers have been reported. It has been also shown that more than 1000 cantilevers can be operated to realize a nanomechanical storage device.[15]

Masking or selective coating with different methods such as incubation into capillary arrays[16] or inkjet deposition[17] have been used to differentiate reference and sensing MCSs. Cross contamination during such masking or coating procedures could happen which in turn would cause cross-talk and interference in the response of neighboring MCS. In this work, we used a new optical reader setup, which is capable of monitoring the deflection of 16 MCSs in parallel. The MCS array layout consists of four separate wells, each containing four MCSs plus a reference mirror. This configuration allows an easy, independent, and automated functionalization by fluidic flow without the risk of cross contaminations among different wells. In addition, cross-talks caused by molecules detaching from sensor or reference coatings, diffusing to adjacent MCSs, are avoided anytime during the measurement. The presence of a reference mirror in each well allows measuring of the absolute MCS bending, which is the deflection of the cantilever's free end relative to its straight position. In addition, the reference mirror can be used to monitor potential optical artifacts such as refractive index changes due to the exchange of solutions in the wells.

In this article, we describe the multiwell micromechani-

[a]Also at Department of Biophysical and Electronic Engineering, University of Genova, via all'Opera Pia 11a, I-16145 Genova, Italy.
[b]Electronic mail: berger@mpip-mainz.mpg.de
[c]Present address: SBCBE, VIT University, Tamil Nadu, India 632 014.
[d]Electronic mail: rr@unige.it
[e]Present address: Nanoscience Instruments, 9831 South 51st St, Suite C119, Phoenix, Arizona.

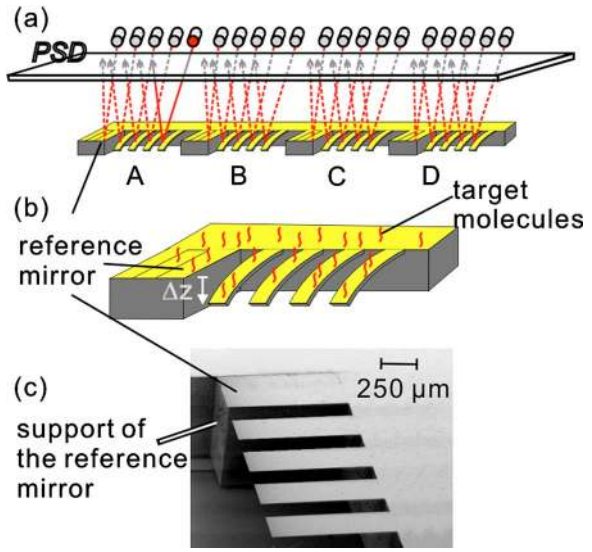

FIG. 1. (Color online) (a) A sketch of the optical laser beam deflection readout system of the MCS array. Shown are the four MCSs and the fixed mirror within the four wells (A, B, C, and D), respectively. The lasers are time multiplexed and the fifth laser in well A is highlighted exemplarily which means it is switched on. (b) MCS bending is induced by the interactions of probe molecules with the sensor coating of MCS. Δz is the value of absolute bending between the reference mirror and the MCS within the well. A positive deflection corresponds to an upward bending. (c) Scanning electron microscope (SEM) micrograph of one well within the MCS array.

cal cantilever array reader performance, the fluidic delivery system, and present the system response upon alkanethiol adsorption.

II. INSTRUMENT DESCRIPTION

A. Cantilever sensor array

The MCS array used in these experiments is composed of sixteen identical rectangular silicon micromechanical cantilevers and four reference mirrors grouped into four separate wells [Fig. 1(a)]. The volume of each well in the fluid cell is 3 μl. The reference mirror can be used to measure the absolute MCS bending by calculating the difference in the output signals of MCS and reference mirror on position sensitive detector (PSD) [Fig. 1(b)]. MCSs are fabricated from single crystal silicon and are 500 μm long, 150 μm wide, and 1 μm thick (Silex Microsystems, Bruttovagen, Sweden) [Fig. 1(c)]. The upper side of each MCS is coated with a 5 nm Ti/W adhesion layer and a 30 nm Au layer. The MCS in each well have a pitch of 250 μm, respectively. The supporting chip is 22 mm long, 5 mm wide, and 500 μm thick. Prior to use, each MCS chip was cleaned by highly reactive ozone generated with a UV lamp (PSD-UV, Novascan Technologies, Inc., IA) for 20 min.[18]

B. Optical readout

MCS deflections are monitored using a new device (Veriscan3000 by Protiveris Inc. Rockville, MD) that utilizes an optical beam deflection readout employing a linear array of vertical cavity surface emitting lasers (VCSELs, wavelength of 760 nm) and an array of microfocusing lenses. The laser spots focused on the MCS free ends are reflected by the gold surface to a linear PSD. The laser power can be adjusted individually for each VCSEL to obtain a desired intensity signal at the PSD. The PSD (20×20 mm^2 sensing area) position can be adjusted with two micrometer screws to achieve an alignment relative to the reflected laser spots. With this design, MCS bending can be measured down to 0.1 nm. The interference on the PSD from the external light can be minimized by housing the whole setup in a closed chamber.

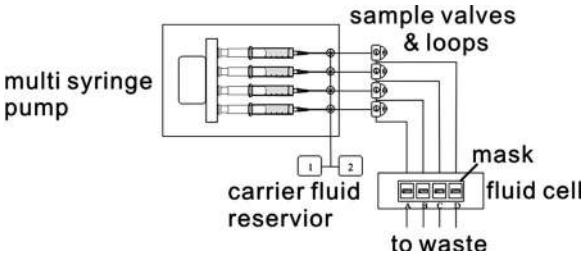

FIG. 2. A schematic outline of the fluidic delivery system for the MCS array.

C. Flow cell and fluidic delivery system

To deliver the carrier fluid and different sample solutions to the MCS array, a syringe pump fluidic system is used. Each well is connected to one syringe, which can then be operated in parallel. The system consists of four valves for the carrier fluid, four syringes, four sample valve loops, four injection valves for sample solution, and one cartridge containing the fluid cell with the four wells (Fig. 2). When the MCS array is mounted in the cell, each well is isolated by a Teflon gasket. This enables the introduction of different carrier fluids and sample solutions into the different wells, thus allowing the parallel analysis of various recognition assays. The whole cartridge containing the flow-through cell can be heated up to 70 °C using a resistor embedded in the metal body of the cartridge itself together with two temperature sensors. The cartridge is thermally insulated from the rest of the device by a thick Teflon sheet. The temperature can be controlled with 0.1 °C precision using an external temperature controller (LakeShore Model 330, Lake Shore Cryotronics, Inc. OH).

A manual valve allows the interchange between two carrier fluids for each of the four fluidic channels. The reservoirs of the syringes have a volume of 2.5 ml. All the syringes are driven by a single stepper motor controlled via software in order to aspirate and dispense carrier fluid to the four wells simultaneously and at the same speed in the range of 0.5–2000 μl/min. Between each syringe and the corresponding well, there is a standard sample injection loop made of polyethylether ketone (PEEK). The volume of the sample loop can be selected in a range of 20–2000 μl. The loop is connected to a six-port injection valve which is used to interchange the flow stream. With the injection valve at "load" position, sample solution can be loaded into the loop without flowing to the fluid cell and disturbing the carrier fluid flow. After switching the injection valve to "inject" position, the carrier fluid flows through the loaded loop and sample solution is delivered to the fluid cell. Other than the injection loops, all tubings are fluorinated ethylene propylene (FEP).

D. Finite element modelling of the flow

In order to interpret the experimental results, we have modeled and simulated the flow of the solution in a single well using finite element software (COMSOL MULTIPHYSICS by COMSOL Inc., Burlington, MA). The model we used is based on a tetrahedral mesh composed of 17 739 elements. At each mesh node the Navier-Stokes equation was solved in order to calculate the solution speed. Then convection-diffusion equations were solved for calculation of the concentration profile versus time of the analyte solution after injection.

III. RESULTS

A. Calibration

We calibrated the beam deflection detection setup by measuring the absolute bending of the MCS with a white-light confocal microscope (μSurf®, NanoFocus AG, Oberhausen, Germany) at different temperatures. Since the MCS were coated on top with a gold layer, they behave like a bimetallic actuator.[19] Figure 3(a) shows a confocal microscope image of the gold coated side of four MCSs in one well. One can see clearly that the reference mirror remains on the same plane as the surrounding chip. This position is defined as zero nanometers in a profile along the free end of the MCS [indicated by a line in Fig. 3(a)]. At room temperature, all MCSs are bent upwards with respect to the reference mirror. This bending is attributed to the residual stress of the deposited Ti/W/Au layers. For the four MCSs of Fig. 3(a), we measured a displacement of the free end of 5312±1 nm (MCS 1), 5425±1 nm (MCS 2), 5471±1 nm (MCS 3), and 5008±1 nm (MCS 4) relative to the mirror level, respectively. The average deflection within this well was 5304±208 nm. Upon heating the chip to higher temperatures, we observed, as expected, that all MCS bent away from the gold coated side towards the reference mirror [Fig. 3(b)]. By fitting the observed average deflections at five different temperatures, in the range of 25 to 45 °C we found a linear dependence of bending with temperature having a slope of −210 nm/°C. The same chip was then mounted in the Veriscan3000 device with lasers aligned on the end of reference mirrors and free ends of all MCS. The temperature of the chip was ramped from room temperature to 45 °C [Fig. 3(c)]. The bending follows a linear dependence having a slope of −20 arbitrary units/°C. Together with the results from confocal microscope a conversion factor of 10.5 nm/arbitrary unit for the current optical setup was calculated.

B. Resonance frequency

Calculations of differential signals only make sense if the mechanical parameters of MCS in the different wells within one chip are comparable. Therefore, we determined the resonance frequencies of the 16 MCSs by recording oscillation spectra induced by thermal noise. The resonance frequency of each MCS was then obtained by fitting each spectrum with a Lorentzian curve.[20] Resonance frequencies were determined to be 5146±14, 5151±18, 5154±15, and 5159±7 Hz for MCSs in well A, B, C, and D, respectively.

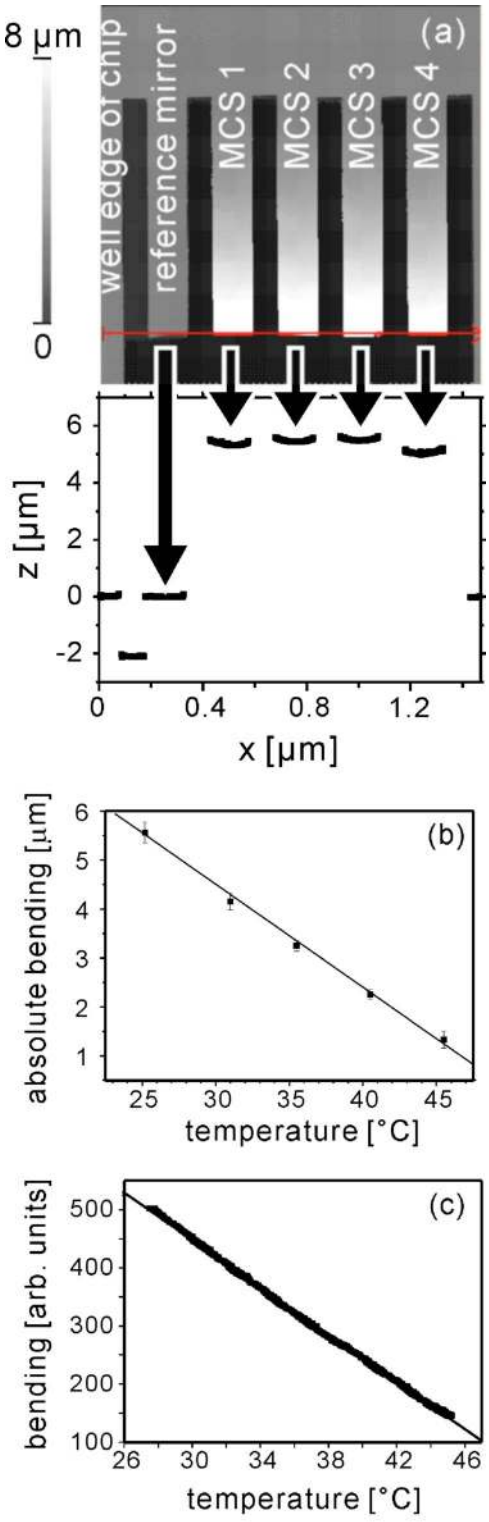

FIG. 3. (Color online) (a) The shape of MCS recorded by white-light confocal microscopy at room temperature (25.2 °C). MCS 1–MCS 4 are bent upward. The reference mirror has the same level than the surrounding chip surface. The red line in this micrograph indicates the position where the MCS bendings were measured. (b) The profile corresponding to the bending of the four MCSs. The differential bending is always defined relative to the mirror position which is defined to be 0 nm. (c) The average absolute bending of all Au coated MCS within one chip upon temperature change. This dependence was measured by the white-light confocal microscopy. (c) The average absolute bending of all MCSs within the same chip upon temperature change measured by the Veriscan3000. The slope of linear fitting is −20 arbitrary units/°C.

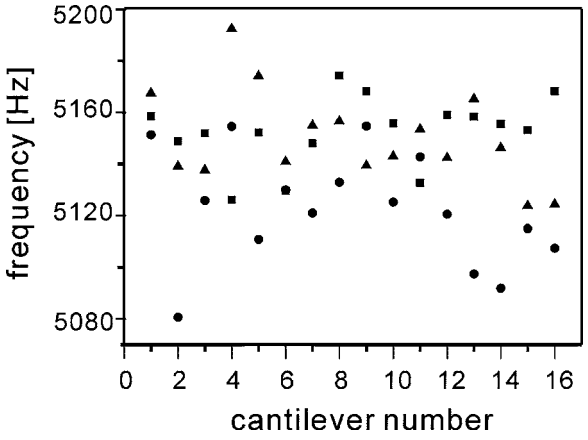

FIG. 4. Resonance frequencies of MCS obtained from thermal tune spectra. For comparison, all 16 MCSs of three arbitrarily chosen chips are plotted. All first resonance frequencies determined vary between 5080 and 5200 Hz. Squares correspond to chip 1, circles to chip 2, and triangles to chip 3.

The small variation $<1\%$ indicates that the mechanical properties of the MCSs are quite similar and are suitable for the differential deflection measurements. In addition, we observed that frequency variations of MCS between different chips are very small, within few percents (Fig. 4 and Table I).

C. Effect of different flow rates

1. Sample entry delay times

For MCS, it is essential to calculate the differential deflection between functionalized and reference sensors in analyte flow in order to compensate unspecific adsorption. In our setup, reference MCSs are situated in different wells connected independently to the fluidic delivery system. The calculation of differential signals between wells leads to reliable data only if both wells are exposed at the same time to the same analyte flow and analyte concentration.

There is always a time delay in the MCS response after sample injection owing to the time the sample solution needs to pass through the tubing and fill the well. This depends on the flow rate and on the tubing volume mainly given by the length. In order to estimate delays for each well, we injected air bubbles in a water flow and monitored the PSD signal. A sudden decrease of the sum signal on the PSD indicated that an air bubble entered the well. The delay volume was calculated to be 147, 143, 146, and 148 μl for wells A, B, C, and D, respectively. These small differences in delay volumes are considered upon calculation of differential MCS response between different wells. In case a flow rate of 5 μl/min is used in an experiment, the delay volume results in a time offset of 48 s of well A relative to well B. This time offset can be subtracted from the measurement time obtained for well B.

2. Flow rate dependence

Typical flow rates for MCS employed in biosensing are between 5 and 100 μl/min.[21] To investigate the effect of different flow rates on the bending behavior of the MCS, we performed experiments by flowing water at different flow rates, e.g., 50, 100, 200, and 300 μl/min [Fig. 5(a)]. The MCS immediately responded to an increase of the flow speed by bending downwards relative to the mirror position, i.e., downwards in Fig. 1.

From these experiments, the deflection jump for each flow rate change, $\Delta D_{\Delta\text{flow}}$, was calculated [Fig. 5(b)]. We conclude, first, that $\Delta D_{\Delta\text{flow}}$ of the MCS increases with increasing flow rates and, second, that the effect of flow rate on $\Delta D_{\Delta\text{flow}}$ is reversible. Thus the flow rate effect is attributed to forces arising from the hydrodynamic flow surrounding the MCS. Consequently, using MCS which have different layout, shape, bending, or higher order of curatures can exhibit different flow rate effects.

3. Flow rate dependence on MCS with different curvatures

The flow rate experiments were repeated with additional three chips to demonstrate the influence of the absolute bending of MCS to its bending changes. Therefore, we have selected MCS chips having a different initial absolute bending at room temperature of 5733, 4742, and 1385 nm in average for chips 1, 2, and 3, respectively [Fig. 5(c)]. The absolute bending direction of all MCS is upward (towards the gold side) relative to the zero level of the mirror. We found that $\Delta D_{\Delta\text{flow}}$ is larger for the MCS of the chip having larger absolute bending, i.e., $\Delta D_{\Delta\text{flow,chip1}} > \Delta D_{\Delta\text{flow,chip2}} > \Delta D_{\Delta\text{flow,chip3}}$. This dependence indicates that there is a more pronounced effect of the flow change on the MCS exhibiting a higher bending.

This effect may sound trivial, but it has consequences for in-flow experiments in terms of differential measurements between reference and sensing MCSs. The sensing and the reference MCSs are composed usually of different surfaces. Since different surfaces can have different surface energies, a different surface stress acts on the MCS. Thus, the initial bending of MCS is already different prior to the sensing experiment. One example is when MCS are coated by a gold layer for thiol immobilization of molecules and reference

TABLE I. Average of the resonance frequency of MCS in each well and average of four wells of each chip. The variation in average value is the standard deviation among MCSs. The percentage of the variation is also given for average of four wells of each chip.

	Average of well A (Hz)	Average of well B (Hz)	Average of well C (Hz)	Average of well D (Hz)	Average of four wells (Hz)
Chip 1	5146±14	5151±18	5154±15	5159±7	5151±18 (0.35%)
Chip 2	5128±34	5124±10	5136±16	5103±10	5128±34 (0.66%)
Chip 3	5159±26	5157±14	5145±6	5140±20	5153±33 (0.64%)

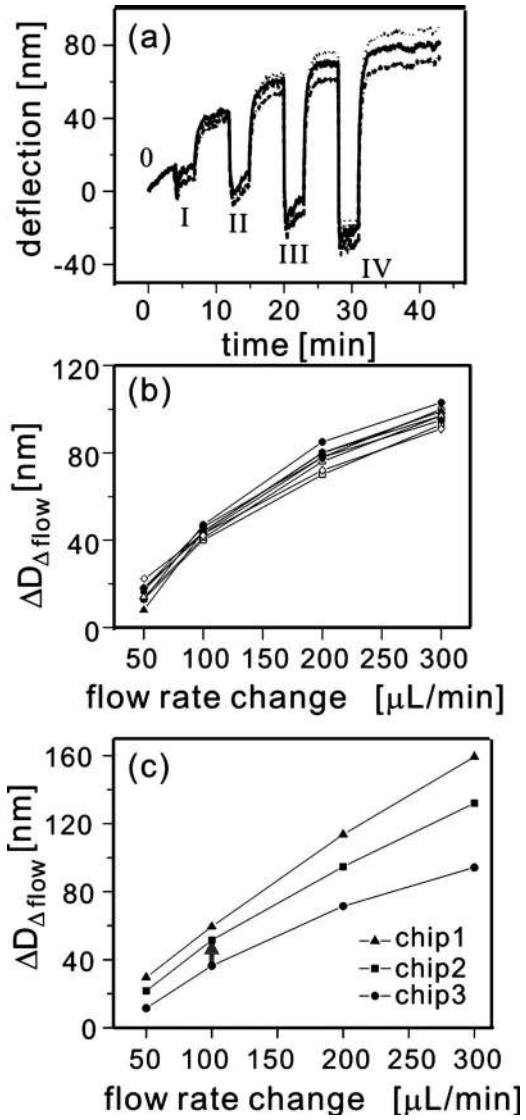

FIG. 5. (a) Bending of the MCS upon water flow at different flow rates. The traces are the average traces of four MCSs in each well. 0 indicates no flow, I a flow of 50 μl/min, II 100 μl/min, III 200 μl/min, and IV 300 μl/min. (b) Jump height $\Delta D_{\Delta flow}$ calculated from the measurement shown in (a) as a function of flow rate. Filled symbols correspond to a flow increase and open symbols to a flow decrease. Squares correspond to well A, circles to well B, triangles to well C, and diamonds to well D. (c) Average jump height of four wells as a function of flow rate for three different chips.

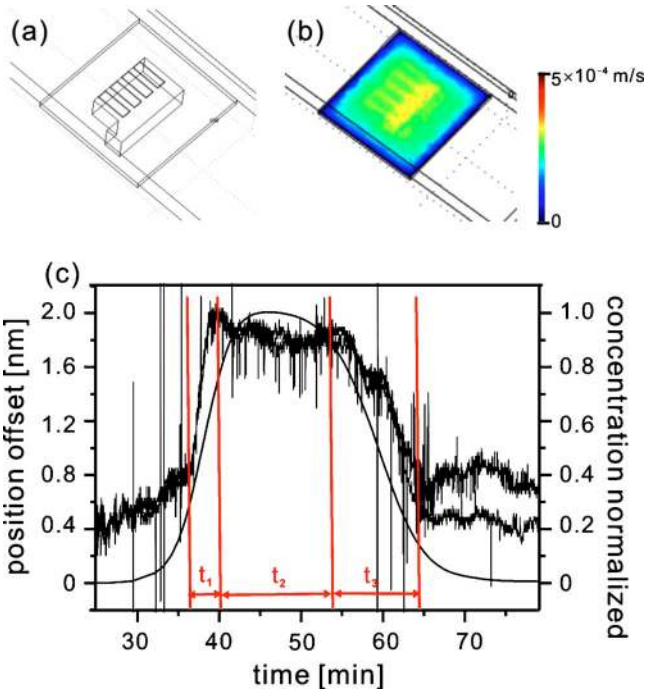

FIG. 6. (Color online) (a) View of one of the four identical flow-through measurement chambers. (b) Stationary velocity field of the flow-through chamber obtained by finite element simulation. The color scale corresponds to ranges from 0 to 5×10^{-4} m/s. (c) Two exemplary position offset signals upon exchange of water with BSA water solution. The solid line represents the simulated concentration dependence for the same experiment. Three regions can be distinguished: a first interval t_1 where the normalized concentration reaches the maximum, a second interval t_2 where only the analyte BSA water solution is present in the cell, and a third interval t_3 where the analyte solution is washed away by the water carrier fluid.

MCS stay uncoated. The Au coating process is known to result in a bending of MCS.[22] In this case, a change in the flow speed would induce a "parasitic" differential deflection. Consequently, MCS experiments should always be performed or compared which were recorded at a constant flow rate.

Of course, since the measurement of the MCS bending is fundamental and it is the quantity to be measured upon exposure to an analyte, the influence of the absolute bending in an experiment must be considered even at constant flow. Upon binding of molecules to a MCS surface, bending of several micrometers were reported.[23] To illustrate the influence of hydrodynamic flow induced response on MCS, an initial absolute bending of the MCS of approximately 1400 nm is assumed. In addition, we assume that the binding of molecules leads to a bending change of 3300 nm. The difference in hydrodynamic flow induced bending would be in the order of 15 nm [see gray arrow in Fig. 5(c)] or around 0.5%, which can be considered as negligible. However, the above measurements and considerations demonstrate that measurements of the absolute bending of MCS lead to a more detailed understanding of its sensing mechanisms and can improve the reliability of the obtained experiment.

D. Mixing of solutions during sample injection

When dealing with adsorption kinetics, it is important to know not only the delay between sample injection and introduction into the measurement chamber but also the mixing behavior of the analyte and carrier fluid inside the entire fluidic system. Here, we consider the measurement chambers, consisting of an inlet, outlet, and the chip well with the four MCSs and the reference mirror, as depicted in Fig. 6(a). Finite element simulations revealed the flow profile within a well [Fig. 6(b)].

As a model of analyte/carrier fluid, we used a bovine serum albumin (BSA) solution (5 mg/ml) and de-ionized (DI) water. To increase the effect of refractive index changes on the displacement of the reflected laser beams, we tilted the cartridge hosting the MCS array. To be sensitive to changes in refractive index only, all laser spots were focused on the rigid chip surface (instead of the free end of the cantilever). Thus, recorded deflection signals do not correspond to a real deflection. Therefore, we referred to this signal as

position offset. In the beginning, the wells were filled with de-ionized water at a constant flow rate of 10 μl/min. Under these conditions, the position offset is attributed to a BSA concentration of 0. Thereafter a BSA water mixture in wells B and D was introduced and the position offset was monitored [Fig. 6(c)]. The position offset increased, owing to an increase in refractive index upon switching from water to the BSA solution. The injection of the BSA water solution resulted in a transition time of 3 min, corresponding to a volume exchange of 30 μl in wells B and D. After that, the position offset reached a constant value, which is attributed to a constant concentration of the BSA water mixture (13 min or a flow volume of 130 μl). Then the BSA water mixture was exchanged by DI water again. The position offset signal returned to the initial value after 11 min (corresponding to 110 μl volume exchange). In a control experiment, the flow of water alone in wells A and C produced no change in position on PSD signal (not shown here).

The time dependence of the BSA concentration calculated at the free end of the MCS was compared to position offset signal in our refractive index measurement [black solid line in Fig. 6(c)]. The simulation results show good agreement with our experimental observation. The result of the simulation and the experiment indicates that the signal recorded from the reference mirror within one cell can be used to monitor the concentration changes owing to mixing effects in each well.

E. Thiol adsorption experiment

To evaluate the performance of the MCS array to molecular interactions, we conducted thiol adsorption experiments using 6-mercapto-1-hexanol (MCH). The Au coated MCS were immersed in water at a constant flow rate of 5 μl/min until an equilibrium in the drift of the bending was reached. Then, without stopping the flow, 200 μl MCH solution at the concentration of 1 mM were injected in wells B and D followed by water again to remove unbound MCH molecules from the MCS surfaces. The initial absolute bending of Au coated MCS, due to residual stresses, is of few micrometers upward relative to the reference mirrors (i.e., toward the gold side), as can be observed in the graph of Fig. 7(a). Upon MCH exposure of the MCS in wells B and D, the deflection decreases significantly by around 600 nm towards the reference mirrors.

To compare the signals, which were recorded in the different wells, the average deflection signals in each well were calculated. Then the signals recorded from reference wells A and C were subtracted from the signals recorded for wells B and D [Fig. 7(b)]. Hereby, the initial deflection was defined to be zero for all wells. The deflection changes indicate an increase of the compressive stress of the gold coated side[24–26] induced by the self-assembled monolayer on the MCS. A compressive stress means that the gold side of the MCS is expanding relative to Si. The maximum deflection of wells B and D are 688±5 and 662±5 nm, respectively. This indicates that the coverage of MCS surfaces by MCH molecules is similar for both wells. After water rinsing through the cell, the deflection signals show a slight variation, within 10 nm, which indicates that mainly immobilized MCH molecules contribute to the observed bending. The control experiments were performed by water flow in wells A and C. The deflection changes in these two reference wells were observed to be $<$80 nm.

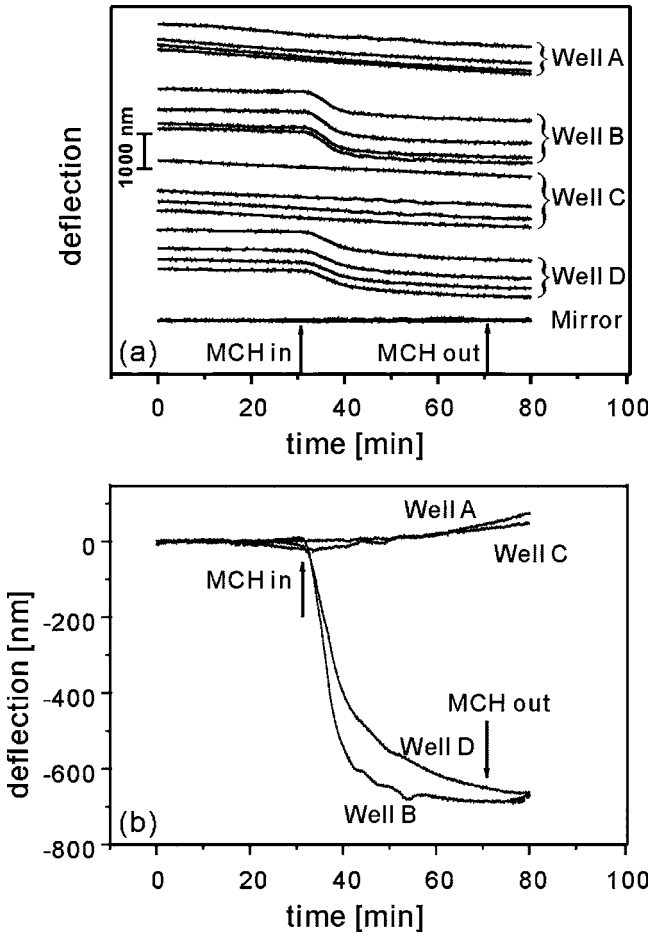

FIG. 7. (a) Deflection of all MCSs for MCH (1 mM) adsorption. De-ionized water was delivered as a carrier fluid. The flow rate was kept at 5 μl/min. At t=8 min MCH was injected in wells B and D. The arrow shows at t=31 min MCH reaching the MCS, and at t=71 min MCH flowing out of the cell. For clarity, we have grouped signals from each well by shifting the deflection offset. (b) Average deflection of four wells calculated from (a). The curves shown in the graph have already been drift subtracted.

IV. SUMMARY

A new optical reader was evaluated for simultaneous monitoring of 16 MCSs for potential use in chemical and biological detections. The array used for the studies comprises of 16 MCSs and four fixed mirrors arranged in four wells. Absolute values of MCS deflections can be recorded. A reversible, linear dependence of MCS bending with fluid flow rate was observed. One of the main advantages of the described multiwell micromechanical cantilever array reader is the simplified functionalization procedure of MCS, which can be performed simply by flowing individual fluids or gases through a selected well. Therefore, standard protocols for surface functionalization can be applied and no further equipment is required. The latter compatibility to standard protocols is highly required in the field of biotechnology.

ACKNOWLEDGMENTS

The authors acknowledge the partial support from the DAAD (Vigoni D/04/42051). Hans Jürgen Butt, Elmar Bonaccurso, Maren Müller, Yajun Cheng, and Gunnar Glasser (MPI-P) are acknowledged for fruitful discussions and continuous support.

[1] J. K. Gimzewski, Ch. Gerber, E. Meyer, and R. R. Schlittler, Chem. Phys. Lett. **217**, 589 (1994).
[2] R. Raiteri, G. Nelles, H.-J. Butt, W. Knoll, and P. Skládal, Sens. Actuators B **61**, 213 (1999).
[3] R. McKendry *et al.*, Proc. Natl. Acad. Sci. U.S.A. **99**, 9783 (2002).
[4] S. Cherian, R. K. Gupta, B. C. Mullin, and T. Thundat, Biosens. Bioelectron. **19**, 411 (2003).
[5] A. Johansson, G. Blagoi, and A. Boisen, Appl. Phys. Lett. **89**, 173505 (2006).
[6] M. Sepaniak, P. Datskos, N. Lavrik, and C. Tipple, Anal. Chem. **74**, 568a (2002).
[7] V. Tabard-Cossa, M. Godin, P. Grütter, I. Burgess, and R. B. Lennox, J. Phys. Chem. B **109**, 17531 (2005).
[8] Y. Arntz *et al.*, Nanotechnology **14**, 86 (2003).
[9] S. H. Lim, D. Raorane, S. Satyanarayana, and A. Majumdar, Sens. Actuators B **119**, 466 (2006).
[10] F. Huber, M. Hegner, Ch. Gerber, H.-J. Güntherodt, and H. P. Lang, Biosens. Bioelectron. **21**, 1599 (2006).
[11] H. P. Lang *et al.*, Appl. Phys. Lett. **72**, 383 (1998).
[12] A. Boisen, J. Thaysen, H. Jensenius, and O. Hansen, Ultramicroscopy **82**, 11 (2000).
[13] B. H. Kim, F. E. Prins, D. P. Kern, S. Raible, and U. Weimar, Sens. Actuators B **78**, 12 (2001).
[14] H. P. Lang *et al.*, Anal. Chim. Acta **393**, 59 (1999).
[15] A. Knoll *et al.*, Microelectron. Eng. **83**, 1692 (2006).
[16] B. Dhayal, W. A. Henne, D. D. Doorneweerd, R. G. Reifenberger, and P. S. Low, J. Am. Chem. Soc. **128**, 3716 (2006).
[17] A. Bietsch, J. Y. Zhang, M. Hegner, H. P. Lang, and Ch. Gerber, Nanotechnology **15**, 873 (2004).
[18] J. R. Vig, J. Vac. Sci. Technol. A **3**, 1027 (1985).
[19] R. Berger, Ch. Gerber, H. P. Lang, and J. K. Gimzewski, Microelectron. Eng. **35**, 373 (1997).
[20] R. Lévy and M. Maaloum, Nanotechnology **13**, 33 (2002).
[21] X. R. Zhang and X. F. Xu, Appl. Phys. Lett. **85**, 2423 (2004).
[22] J. Mertens, M. Calleja, D. Ramos, A. Tarýn, and J. Tamayo, J. Appl. Phys. **101**, 034904 (2007).
[23] F. Zhou, W. M. Shu, M. E. Welland, and W. T. S. Huck, J. Am. Chem. Soc. **128**, 5326 (2006).
[24] R. Berger, E. Delamarche, H. P. Lang, Ch. Gerber, J. K. Gimzewski, E. Meyer, and H.-J. Güntherodt, Science **276**, 2021 (1997).
[25] R. Raiteri, H.-J. Butt, and M. Grattarola, Electrochim. Acta **46**, 157 (2000).
[26] J. Fritz *et al.*, Langmuir **16**, 9694 (2000).